Journal of Hydrology 603 (2021) 127015

Contents lists available at ScienceDirect

Journal of Hydrology

journal homepage: www.elsevier.com/locate/jhydrol

Research papers

Comparison of fiber-optic distributed temperature sensing and high-sensitivity sensor spatial surveying of stream temperature

Ruba A.M. Mohamed [a], Chris Gabrielli [b], John S. Selker [b,c], Frank Selker [b], Scott C. Brooks [d], Tanzila Ahmed [a], Kenneth C. Carroll [a,*]

[a] Department of Plant and Environmental Sciences, New Mexico State University, P.O. Box 30003, Las Cruces, NM 88003, USA
[b] Selker Metrics, 4225 SW Agate Lane, Portland, OR 97239, USA
[c] Department of Biological & Ecological Engineering, Oregon State University, Corvallis, OR 97331, USA
[d] Environmental Sciences Division, Oak Ridge National Laboratory, P.O. Box 2008, MS 6038, Oak Ridge, TN 37831-6038, USA

ARTICLE INFO

This manuscript was handled by Corrado Corradini, Editor-in-Chief, with the assistance of Nick Engdahl, Associate Editor

Keywords:
Hyporheic
Fiber-optic distributed temperature sensing
Distributed Temperature Sensing
DTS
Stream temperature
Temperature sensor

ABSTRACT

Measuring surface water temperature spatial variability is needed to estimate the interaction between surface water and groundwater, evaluate fish habitat and thermal inertia, and to estimate streamflow frequency and duration. Fiber optic distributed temperature sensing (FO-DTS) has been used in rivers and lakes, providing high-resolution and sensitive temperature monitoring over large temporal and spatial scales. However, in streams with cobbly or bedrock-lined streambeds and variable bathymetry, use of FO-DTS to measure temperature close to the surface water and groundwater interface can be challenging if even feasible. FO-DTS can also be costly, involve difficult installations, and require an advanced understanding of the technology, calibration, and data processing. In this study, we compared FO-DTS stream temperature survey results to an alternative temperature survey method employing a towed transect of high-resolution temperature loggers spaced at 1-m and transported in the stream along the study reach, to measure the spatial distribution of stream-water temperature in East Fork Poplar Creek near Oak Ridge, Tennessee, USA. We assessed the applicability and limitations of the two methods, and quantitatively compared in-situ temperature survey results measured simultaneously with each method. Regression results showed strong temporal and spatial correlation between the two methods. Differences were only elevated near the stream banks in areas that were coincident with correlation slope deviations from unity, which was attributed to shallower water and lower data density. Kriging standard errors were also low at channel center with minor increases near the stream banks. The results suggested that the array of the individual temperature sensors can provide a practical alternative to FO-DTS for thermal characterization of surface water, providing slightly lower spatial and temporal resolution, but with higher accuracy of temperature measurement, with greater simplicity, and with a broader range of conditions where it may be applied.

1. Introduction

Quantification of the interactions between surface water and groundwater facilitates management of water resources and maintains the health of riparian ecosystems (Bertrand et al., 2014; Conant et al., 2019). The bidirectional interaction is important in controlling the transport and fate of contaminants and nutrients, evaluating ecosystem habitat, enhancing thermal refugia and metabolism of benthic community, and controlling the discharge and water-level fluctuations, thermal buffering, and biogeochemical reactions in water bodies. Temperature differential measurement was introduced as a method to estimate groundwater-surface water interaction in the early 1960s (Sorey, 1971; Stallman, 1965). It has also been used in streams and lakes to delineate flows in the hyporheic zone, to estimate depth to salt-water interface, and to estimate parameters for heat flow models. Temperature is considered a relatively robust and inexpensive parameter to measure in surface water systems, and the distinctive difference between surface water and groundwater temperatures have allowed for the identification of locations with colder or warmer seeps that may be attributed to groundwater influx (Stoneman and Constantz, 2003; Winter et al., 1988). Measurement of temperature gradients and hydraulic gradients in at least two depths in the sediments are required to estimate the rate

* Corresponding author.
E-mail address: kccarr@nmsu.edu (K.C. Carroll).

https://doi.org/10.1016/j.jhydrol.2021.127015
Received 18 June 2021; Received in revised form 21 September 2021; Accepted 25 September 2021
Available online 30 September 2021

of heat transfer through the streambed, and methods to measure temperature at a fine spatial resolution are often needed. Lateral spatial temperature distributions measured at one depth of the stream or streambed sediment may also be used as a boundary condition in analytical solutions to the one-dimensional heat transport equation (Keery et al., 2007; Kurylyk et al., 2019; Schornberg et al., 2010; Scotch et al., 2021). Measurement of the temperature at the sediment interface was also used to estimate the flow frequency and duration in temporary or intermittent streams (Assendelft and van Meerveld, 2019; Constantz et al., 2001; Shanafield et al., 2021). Deployment of a series of temperature probes along ephemeral channels have permitted the determination of the spatial and temporal pattern of streamflow facilitating estimates of stream flow frequency duration, travel time, and transmission losses (Constantz et al., 2001). Spatial stream temperature at variable depths has also been used in fisheries to evaluate thermal enertia and to study the connection between the spatial distribution of fish and locations of seeps in rivers and lakes (Collier, 2008; Fullerton et al., 2018; Huff, 2009). The distribution of fish and their spawning and metabolism and overall growth rates are directly affected by the temperature that surrounds them (Bond et al., 2015). Thermal refugia are critical to the survival of fish during summer months, during extreme warming events, especially in arid and semi-arid regions (Caldwell et al., 2020).

Three main methods have been used to map spatial stream-temperature distributions including direct measurment using temperature sensors, fiber optic distributed temperature (FO-DTS), and remote sensing thermal infrared imaging (TIR) (Coluccio and Morgan, 2019; Conant, 2004; Constantz, 2008; Dzara et al., 2019; Hall et al., 2020; Marruedo Arricibita, 2018; Selker et al., 2006a). Temperature mapping using temperature sensors is an older method that has been known to be simple and inexpensive. However, can be limited spatially and temporally compared to FO-DTS and TIR, and it can be challenging depending on reach size and flow conditions (Conant, 2004; Gendaszek, 2011; Lautz et al., 2010; Lee, 1985; Vaccaro and Maloy, 2006; White et al., 1987). Initiation and use of FO-DTS for more than a decade to map the horizontal temperature distribution in surface water systems has reduced the need for point measurments to map temperatures (Selker et al., 2006a; Selker et al., 2006c). FO-DTS has been used to quantify contaminant and nutrient exchange and transport in the hyporheic zone as well as to estimate vertical fluid velocities, and to monitor temporal changes in fluid flow using heated and non-heated fiber optic reference cables (Kurth et al., 2013; Read et al., 2014; Selker et al., 2006b; Tyler et al., 2009). FO-DTS can generally provide high spatial and temporal resolution, sensitive temperature monitoring, fast thermal response, and consistent accuracy along the cable due to its integration as a single unified system that obviates separate calibration of multiple temperature sensors (Selker et al., 2006a; Selker et al., 2006c; Suárez et al., 2011). FO-DTS has been found to have some limitations in measuring the temperature in surface water systems (Roshan et al., 2014). Solar energy penetrating through the water column can thermally affect FO-DTS measurements (Neilson et al., 2010). Mobile bed material can either bury the cable or separate it from the bed, complicating data interpretation (Sebok et al., 2015). Implementing FO-DTS can also be expensive, time consuming, and logistically challenging with increased technical complexity both in installation and in post-processing compared to most temperature logging sensors (Folegot, 2018). FO-DTS temperature calibration is based on upstream and downstream temperature reference coils (i.e. hot bath and cold bath). Therefore, fluctuations in the temperature of the reference baths can result in calibration complications, and may alter the precision of the cable (Tyler et al., 2013).

Remote sensing TIR has been used to map surface-water temperature and to identify hyporheic zone interactions (Culbertson et al., 2013; Hare et al., 2015; Liu et al., 2016). Success with TIR methods to measure temperature anomalies in the surface water bed is largely affected by the depth of water and the discharge (Dugdale, 2016; Hare et al., 2015; Torgersen et al., 2001). Hare et al. (2015) found that a depth of less than 0.05 m and stream discharge range 0.002–0.2 m^3/s were suitable to detect seepage thermal signature due to reduced thermal stratification in the water column. TIR provides a large spatial coverage of stream and streambed temperature, but generally in a snapshot of time, which limits the understanding of the diurnal effect on stream or streambed temperature (Marcus, 2012; Markus and Helena, 2002; Torgersen et al., 2001). It is also difficult to ascertain if seepage flux occurs along the entire reach length or whether downstream temperatures are influenced by the upstream seepage source. Additionally, TIR imagery can introduce an error in estimating stream or streambed temperature due to the effect of camera distortion and the surrounding environmental conditions at the time of acquisition (Dugdale et al., 2019; Pai et al., 2017). The TIR method may underestimate or fail to detect downwelling flux of surface water to groundwater, which suggests the need for a direct temperature measurement especially in streams where downwelling loss is dominant or the upwelling flux is weak (Dole-Olivier et al., 2019).

Several studies have compared TIR to FO-DTS to evaluate the horizontal spatial distribution of the temperature measurments (Dzara et al., 2019; Hare et al., 2015); however, to our knowledge this is the first study that has compared the horizontal spatial stream-temperature surveys using FO-DTS method and highly sensitive individual temperature sensors within similar spatial and temporal setting. Some studies deployed FO-DTS cables with temperature loggers that had much lower accuracy (compared to those used herein) and a lower spatial coverage compared to the fiber optic cable (Briggs et al., 2016; Lowry et al., 2007; Mamer and Lowry, 2013). Although FO-DTS has been utilized successfully to evaluate the horizontal temperature distribution along streams and lakes (Selker et al., 2014), the FO-DTS method can be challenging at best to implement in streams with bedrock-lined streambed channels and variable streambed bathymetry, which emphasizes the need for a point measurement method as a complementary or a substitute for the FO-DTS method.

The purpose of this investigation was to develop and evaluate a simple array of highly-sensitive temperature sensors to measure the spatial temperature distribution within a natural stream reach. Evaluation of the thermal sensors spatial survey was through direct comparison to a survey method using FO-DTS within the identical study reach area by identifying co-located measurement locations within the data sets of each method, which was implemented near station 5.4 K in East Fork Poplar Creek (EFPC), Tennessee, USA. The methods were compared to evaluate their capabilities, limitations, strengths, and weaknesses of these methods, and to highlight situations in which one or the other might be a better instrument choice for monitoring or surveying stream temperatures.

2. Methods

2.1. Study site

The temperature surveys were both conducted and compared along a ~ 250 m long reach, with an average 13 m width, of EFPC near Oak Ridge, Tennessee, USA (Fig. 1). EFPC is a third order stream characterized with partially-exposed limestone bedrock, variable stream bathymetry, and a thin veneer of sediment (about 20–60 cm deep) overlying the bedrock in most but not all locations of the study reach (Rucker et al., 2021; Mohamed et al., 2021). The study reach is located in a densely forested freshwater emergent wetland with native sycamore, boxelder, and green ash trees, providing heavy canopy cover during summer months (Cunningham and Pounds, 1991). Starting in the early 1950s, EFPC received contaminated flows with mercury and other hazardous metals, affecting the creek water, sediments, and the floodplain along the creek (Brooks and Southworth, 2011). Water quality in EFPC has improved substantially over the past decades, but mercury contamination in the creek remains a persistent problem. Research over the past several years demonstrates that diffuse legacy sources of

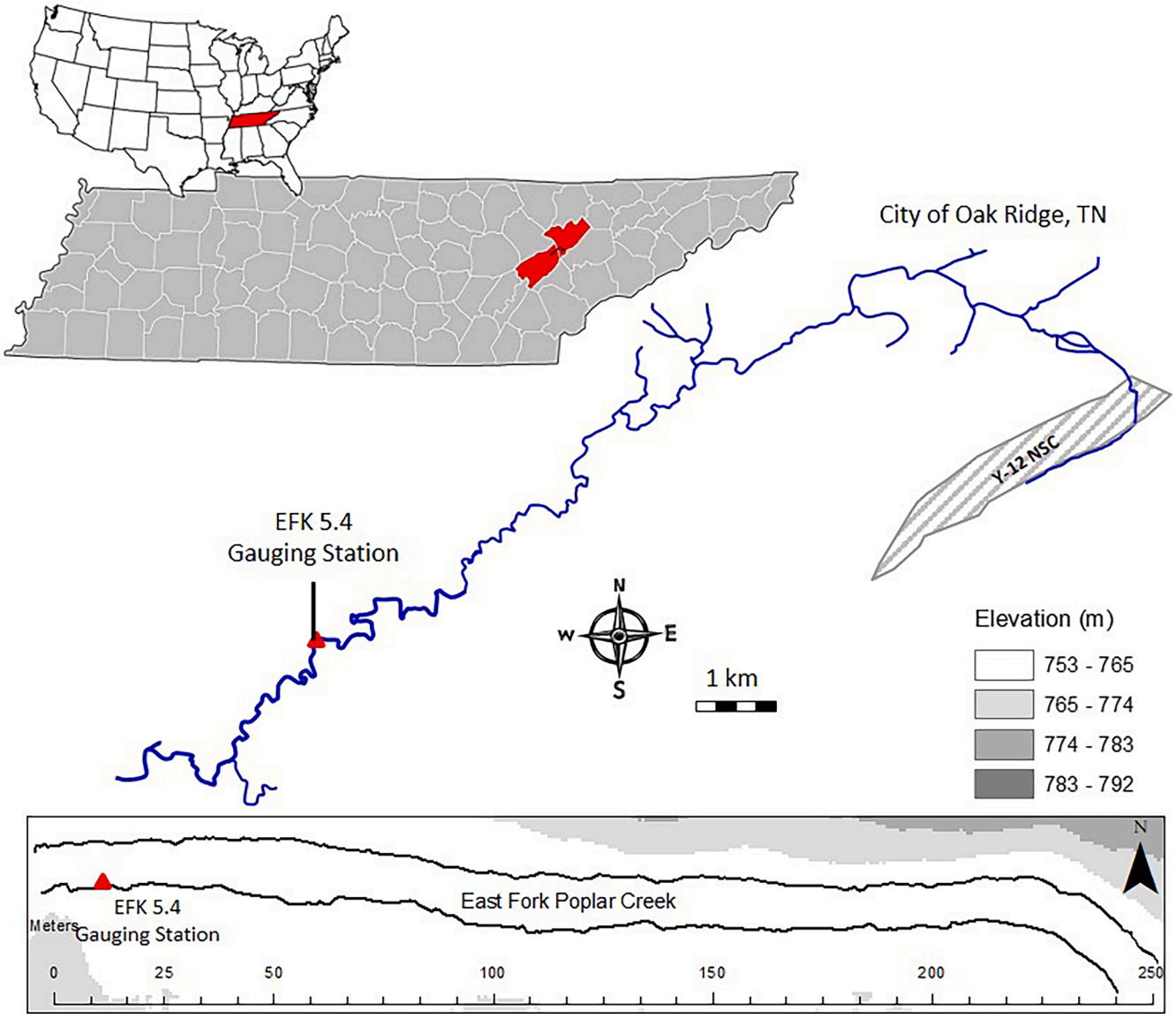

Fig. 1. Maps illustrating the study site location along the East Fork Poplar Creek at station 5.4 km.

mercury contribute to the contaminant load in the creek and that hyporheic water discharging to the surface may be an important source of that increased mercury loading (Brooks et al., 2018; Demers et al., 2018).

2.2. Surveying of measurement locations

The temperature study was conducted during August 2019. Prior to the temperature measurement, the creek banks were surveyed and georeferenced, to allow for spatial referencing of the temperature measurements. The banks were marked with landscape stakes at 1-m intervals along the banks. The distance across the stream between the opposite stakes was roughly the shortest distance between the two banks (i.e. perpendicular to the stream thalweg). The location of the stakes were surveyed with a Leica total station TS02 (Distance measurement with reflector: 1.5 mm + 2.0 ppm and Distance measurement without reflector: 2 mm + 2 ppm) with lowest accuracy in the measurement direction as ± 2.5 mm.

2.3. Discrete upstream and downstream temperatures

In the morning of August 6, 2019, prior to the stream temperature survey, a set of two temperature sensors were placed at fixed locations near the upstream reach boundary, another set of two sensors were placed near the downstream reach boundary, and within each set included one sensor fixed in the stream-water column and another sensor buried in the sediment at about 0.3 m below the top of the streambed. The purpose of these sensors was to provide temporal-monitoring control measurements of the temperature at those locations before and throughout the spatial temperature survey from 16:00 to 18:50 in the same day. Weather data was obtained from a U.S. Department of Energy (DOE) operated meteorological tower (Tower "L") located about 5.75 km southwest of the study site.

2.4. Temperature sensor setup

Six high-sensitivity temperature sensors (model RBR Solos^3 T) were used to survey the spatial temperature variability along the EFPC study reach (Fig. 2). The reported accuracy of the sensors was ± 0.002 °C with a stability of 0.002 °C/year (ITS-90 and NIST traceable standards), with

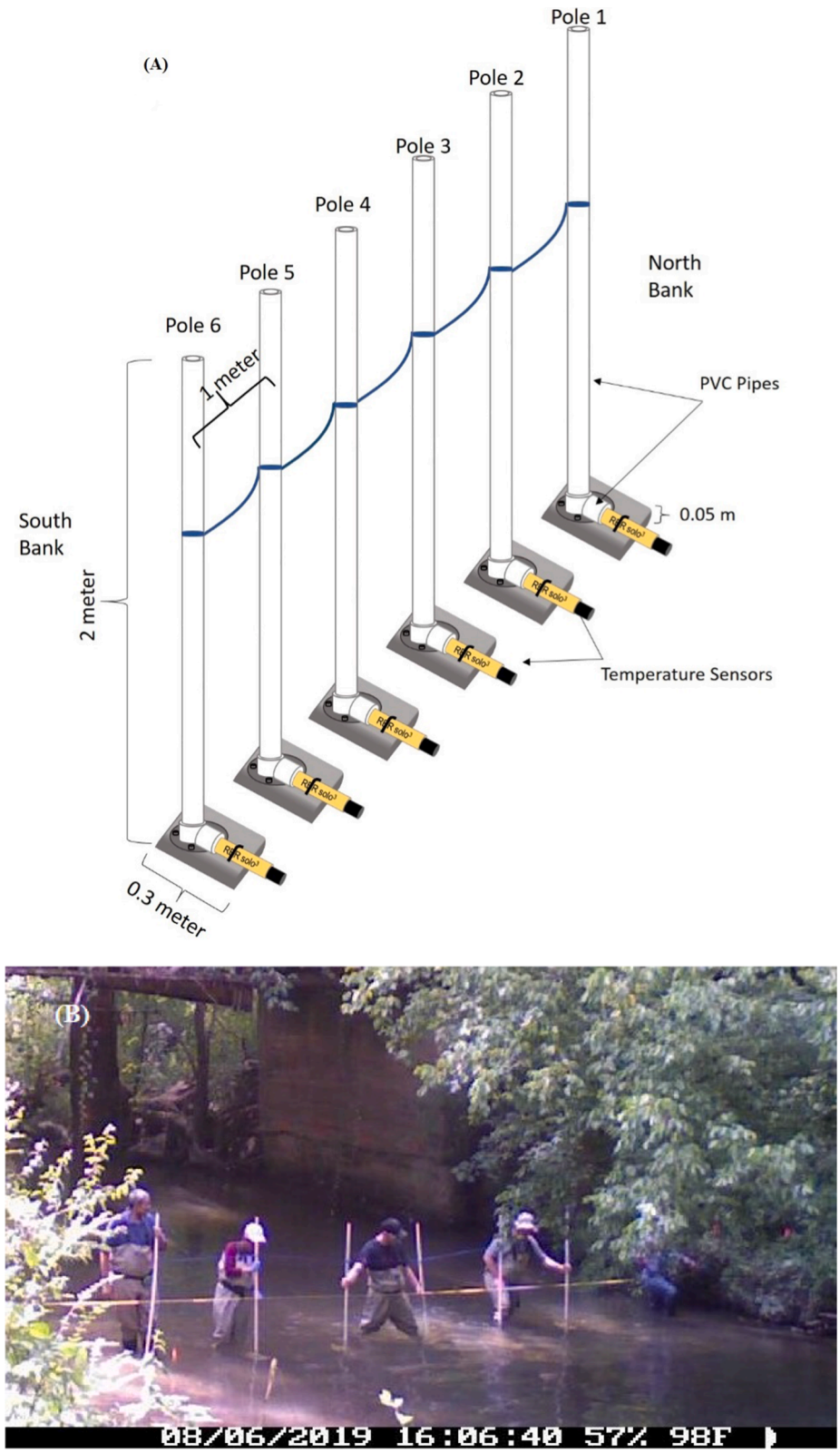

Fig. 2. Illustrative design of the thermal sensor array on the poles connected by 1-m long rope (A), and photograph of the temperature sensor array (B) during operation of the in-stream temperature survey conducted by a 6 person team moving the poles from downstream to upstream while measuring temperatures every 1-m along the stream reach length.

response time of 0.1 s. The absolute accuracy of the sensors used in this study ranged between ± 0.004 °C and ± 0.012 °C, based on the calibration year. Each temperature sensor was attached to a support box at the bottom of a 2.54-cm diameter PVC pipe (hereafter termed poles) (Fig. 2a). The six poles were oriented vertically to position the sensor within the stream at 0.05-m above the top of the streambed to allow for measurement of the stream temperature. The sensors were then spaced in a straight line (or transect) at 1-m apart from each other using equal lengths of string. The transect of temperature sensors poles was oriented perpendicular to the channel and stream flow, and was moved during the sensor-array survey along the direction of the channel to measure the temperature distribution along both the lateral and longitudinal directions of the stream channel. Each of the six equidistant poles measured along a line as they were used to move the sensors in the stream channel along the upstream flow direction, with pole-1 as closest to the north bank and pole-6 closest to south bank (Fig. 2b). The number of the dataset collected with the six sensors in the array at 1-second resolution along the entire reach was 61,296. Transect measurements of temperature were collected and recorded every 1-m along the length of the stream reach at the locations of the survey stakes resulting in a 1-m by 1-m grid of streambed temperatures (Fig. 3a). The total number of data points for the sensor-array survey transects was 1554 (the 222, 223, 227, and 228 m locations had trees logs along the bank obstructing measurement). The distance between the stake marks and the edge of the sensor-array survey transects was measured at each measurement location during the survey. The reporting interval for the temperature sensors was 1 s, and the sensors were allowed 6–7 s to equilibrate at each location before taking the measurement. The temperature survey using the temperature sensors started at the downstream end of the reach on August 6, 2019, at 16:00 Eastern Standard Time zone (GMT-5), the time with the highest temperature difference between groundwater and surface water, and ended at the upstream location at about 18:50.

2.5. FO-DTS setup

The physics of the FO-DTS measurement is based on a temperature dependent backscatter light mechanism including Brillouin or Raman backscatter (Selker et al., 2006c). It is possible to achieve sub-meter scale spatial and 0.01 °C thermal precision for measurement cycle times on the order of minutes for cables extending several kilometers (Tyler et al., 2009). The principle of the FO-DTS method is based on releasing a pulse of laser light into the fiber optic cable and monitoring the Raman-backscatter light to estimate the temperature (Selker et al., 2006c). The distance from where the light was reflected is calculated by timing the return time of the laser pulse. Raman-backscatter reflects at a wavelength shorter or longer than the wavelength of the original pulse. The reflection with the longer wavelength is referred to as Stokes backscatter, and has an amplitude that is not temperature dependent. The reflection with the shorter wavelength is called Anti-Stokes backscatter, and has an amplitude that linearly depends on temperature. By measuring the Stokes/Anti-Stokes ratio at different return locations, the temperature of the fiber can be measured everywhere along the cable length.

The FO-DTS cable was mounted on a raft and was installed in the stream on August 5th, 2019, in six passes, back and forth along the length (parallel to the channel) of the study reach, in a zig-zag pattern to approximately equally distribute the cable spatially along both the width (~1-m apart) and length of the study reach (Fig. 3b). An original goal of the study was to measure streambed temperature at a shallow depth within the streambed to locate temperature anomalies within the streambed that may indicate groundwater seeps. However, due to the heterogeneous bedrock geology and variable bed bathymetry of the study reach, burring the fiber optic cable in the sediment was only possible for a short length of the entire 2 km cable (18%) and the majority of the cable was installed at variable depths of the water-column but as close as possible to the streambed sediment (to a depth between 0 and 0.1 m). Thus, minimal cable was buried due to large sections of streambed being composed of exposed bedrock or large cobbles, and buried locations were recorded by GPS (Topcon HyperLite+) and using the surveyed stakes. At the end of each run along the length of the reach, an anchor was placed to support the cable against streamflow, and the anchor was used to support the turn in the cable for the return pass in the opposite direction. The location of the cable along the stream channel was referenced relative to the surveyed stakes and with a GPS, and the cable turn locations at the anchors were also surveyed. Thus, each temperature value was referenced horizontally in 2D. The total number of the independent temperature measurement was 6257 locations along 1934 m of installed cable (Fig. 3b). The FO-DTS interrogator measured the fiber temperature from August 5th until the 14th, 2019. The total number of data points during the time of the temperature survey with the temperature sensors from 4:00 pm to 6:50 pm on August 6 was 56,313. Both ends of the fiber were connected to the FO-DTS interrogator allowing for double-ended measurements. Each channel in each direction was averaged over 10 min resulting in a dataset with a 20-min measurement interval.

Calibration of raw Stokes/Anti-Stokes values to temperature values were completed following the single-end calibration procedure outlined in Hausner et al. (2011) using warm and cold temperature reference baths at the beginning and end of each channel. During the installation of the FO-DTS cable, we encountered some problems associated with

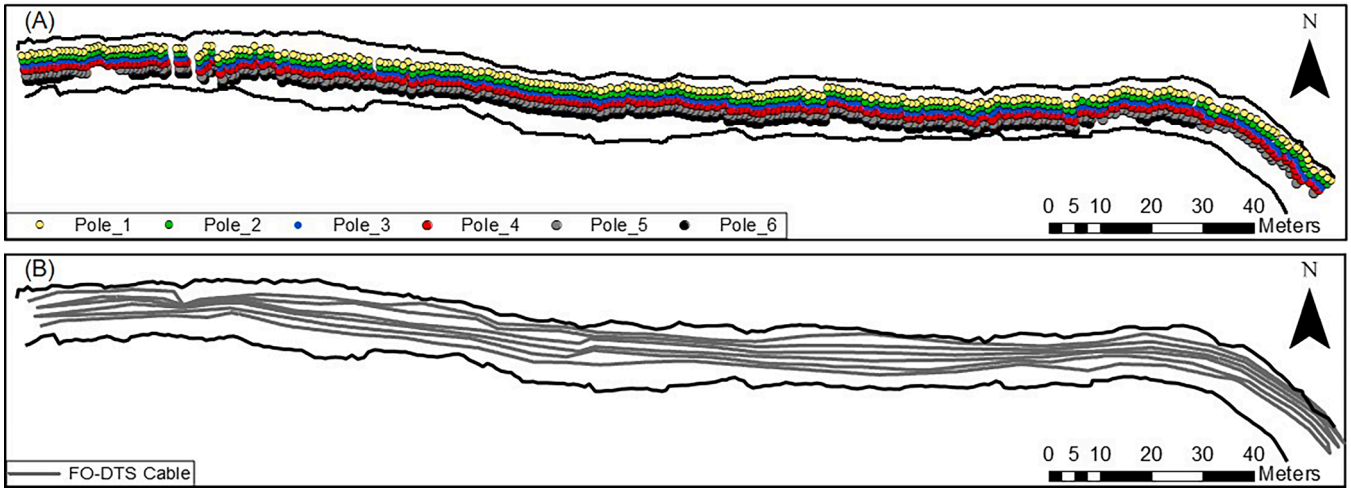

Fig. 3. Map of the temperature sensor measurement locations (A) and the FO-DTS cable (B) data collection locations.

fiber optics and FO-DTS during installation and data analysis. The absolute temperatures estimated with the FO-DTS method had limited accuracy of 0.1 °C in the 20–25 °C range due to several factors including fluctuation of ice baths temperature, which complicated the calibration. Manufacturing and in-stream installation induced strain in the glass fiber created signal artifacts within the length of the cable. To overcome this defect, a calibration procedure was implemented that allowed for the differential attenuation between Stokes and anti-Stokes to vary spatially (Hausner et al. 2011). This reduced the average uncertainty in each observed temperature measurement by 0.07 °C. Although the calibration procedure was successful, it should be noted that there remains a slightly higher level of uncertainty (and thus reduced precision/resolution) in the FO-DTS temperature data than would be found in a typical installation, as the new calibration procedure would not have entirely removed strain induced error in temperature measurements.

2.6. Data analysis

The spatial and temporal scales for the two temperature measurement methods differed, and therefore a number of steps were taken to analyze and compare the two datasets. For the data collected with the temperature sensors, values above the 75th percentile and below the 25th percentile for each sensor was considered an outlier, and was removed from the dataset prior to data analysis and comparison with the FO-DTS dataset. The outliers in this case generally were higher temperature values that indicated the sensor was measuring air temperature in between measurement locations. Eleven outliers were removed from the temperature sensor dataset (i.e. two outliers from pole-1, four outliers from pole-5, and five outliers from pole-6). The total number of temperature measurements after removing the outliers was 1479 (i.e., 255 in pole-1, 259 in pole-2, 259 in pole-3, 259 in pole-4, 244 in pole-5, and 203 in pole-6).

The FO-DTS temperature data were first analyzed to corroborate visual records of fiber optic cable position as either out-of-water, in the water column, or buried within the streambed sediment. Cable position was determined by identifying differences in absolute temperature and variability in hour to sub-daily temperature dynamics at each measurement location. Temperature data recorded by the temperature sensors during the study period on August 6, from 16:00 to 18:50 was compared mainly to fiber locations within the stream-water column (i.e. temperature comparison excluded fiber locations that were either out of water or buried in the sediment), because the thermal sensors measurements were within the stream-water column just above the top of the streambed. Survey data of each temperature sensor measurement and each FO-DTS measurement were used to identify the nearest locational pairs between the two datasets. Data pairs were regressed only if their distance apart was less than 0.5 m (as noted above). To compare temperature data between each matching location pair at similar time stamps, the FO-DTS data was interpolated from 20-min to 1-min data using a splined interpolation approach. Least squares linear regression was used to fit a linear relation between temperature sensor data for each pole and the paired FO-DTS data using Matlab R2021a. R-squared, or coefficient of determination, values provided a goodness of fit for the relationship. A geostatistical analysis was performed for the contour maps of the two temperature methods created using Empirical Bayesian Kriging method using ArcGIS (version 10.5.1). The analysis evaluated the standard error of each prediction and the pixel difference between the two predicted distributions against the accuracy of each temperature method.

3. Results & discussion

3.1. Stream and weather conditions

The timing of the temperature survey was selected between 16:00 and 19:00 to minimize the transient fluctuation in stream and air temperatures. This time also afforded the maximum difference between stream and streambed temperatures, which increased the potential for detection of cooler temperature anomalies associated with groundwater influx. Average air temperature was 24.15 ± 4.84 °C during August 6, 2019, and during the time of the thermal sensors survey (from 16:00 to 18:50) air temperature was relatively constant at 30.7 ± 0.39 °C (Fig. 4). On the day of the temperature survey, the discharge was at baseflow conditions (average value 1.48 ± 0.73 m^3/sec) (Brooks and Lowe, 2019), which allowed the stream discharge to be relatively constant during the time of the spatial survey. The maximum solar radiation was recorded at 14:15 as 1046 W/m^2. The maximum difference between the downstream stream-water and sediment temperatures was 1.3 °C at 16:00, when air temperature and stream-water column temperature were the highest during the day.

The hourly average stream-water temperature gradually increased from 08:00 to the end of the spatial survey measurement at 18:50 (Fig. 4), following the general trend of air temperature. The trend of the stream-water diurnal temperatures in the downstream and upstream boundaries of the study reach were very similar. However, stream-water temperature at the downstream was consistently warmer than the upstream with a maximum difference of 0.12 °C recorded at 14:00, which decreased by the end of the survey at 18:50 with 0.081 °C and 0.03 °C at the downstream and upstream study reach boundaries, respectively. The higher downstream temperature values are explained by warming of the stream as the water flows through open-canopy sections from upstream to downstream during the day.

The diurnal variation of the temperatures within the streambed sediments in the upstream and downstream study reach boundaries were slightly different (Fig. 4). As the stream-water temperature in the downstream was consistently warmer than the upstream, we expected the sediment temperatures to follow the same trend. However, the downstream sediment temperature was consistently lower than the upstream, and remained relatively stable throughout the day. The upstream sediment temperature increased during the day, suggesting possible percolation of warm stream water into the sediment, causing the increase in temperature values.

3.2. Comparison between the temperature sensor and FO-DTS measurements

3.2.1. Raw datasets

Fig. 5 presents the spatial distribution of the measurement locations and the values for the measured temperature at each location for both the thermal sensors (Fig. 5a) and the FO-DTS (Fig. 5b). The temperature trend in Fig. 5b closely followed the trend in Fig. 5a with higher temperature values mostly in the downstream and lower values in the upstream. The maximum temperature recorded with the temperature sensors at 16:45 was 24.00 °C, and the minimum upstream temperature recorded at 18:49 was 23.82 °C. The difference between the maximum and minimum values (0.18 °C) was significant, because it was higher than the accuracy and resolution of the temperature sensors and the FO-DTS methods, and these results were consistent with those presented in Fig. 4. The maximum temperature measured with the FO-DTS method at 16:22 was 24.07 °C, and the minimum temperature measured at 18:50 was 23.72 °C. The difference between the maximum temperature value measured with the FO-DTS method and that measured with the temperature sensors was 0.06 °C, and the difference between the minimum temperature measured with the FO-DTS method and that measured with the temperature sensors was 0.1 °C. These differences were within the accuracy of the two methods (0.4 to 0.1 °C), which suggested that these differences were not substantial. Higher temperature values were recorded with both methods in the downstream relative to the lower values in the upstream portions of the study reach, and the higher temperature values in the downstream were attributed to warming of the stream water as it flowed from upstream to downstream, passing through locations with less canopy cover during measurement time

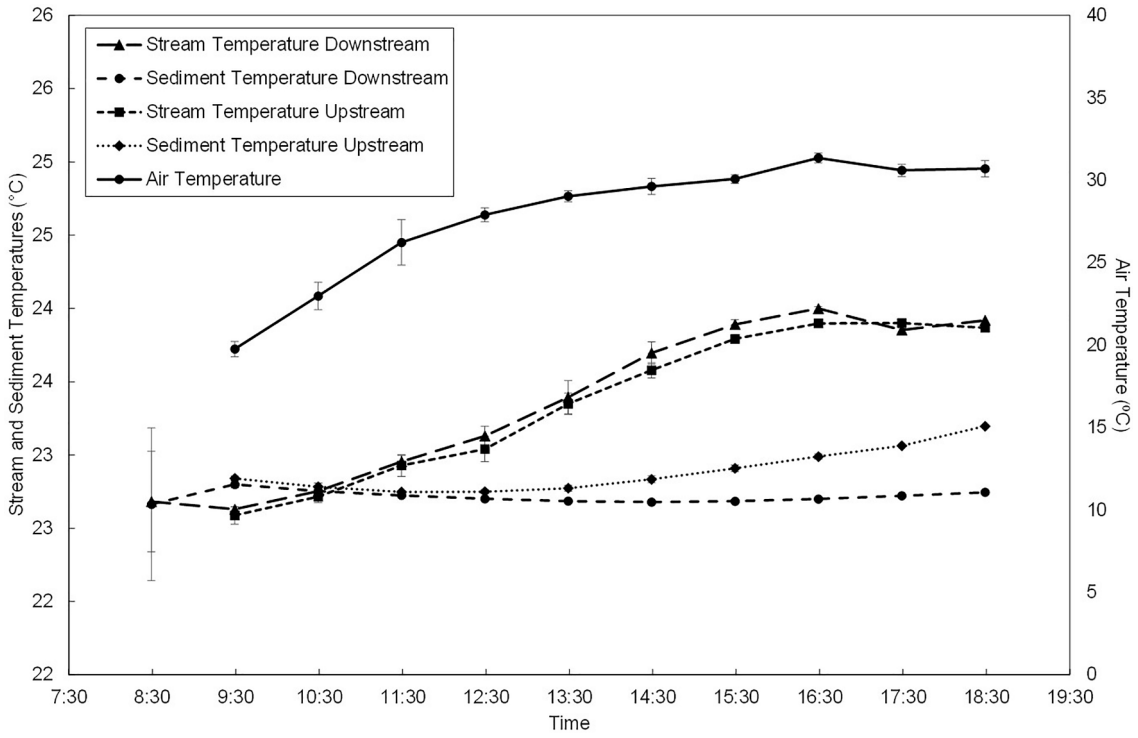

Fig. 4. The hourly average temperature variability of the water-column (i.e., in stream) and sediment (i.e., in streambed) measured in the upstream and downstream using temperature sensors, and the hourly average air temperature variability is also plotted for comparison (all measured on August 6, 2019). Whiskers represent the standard deviation.

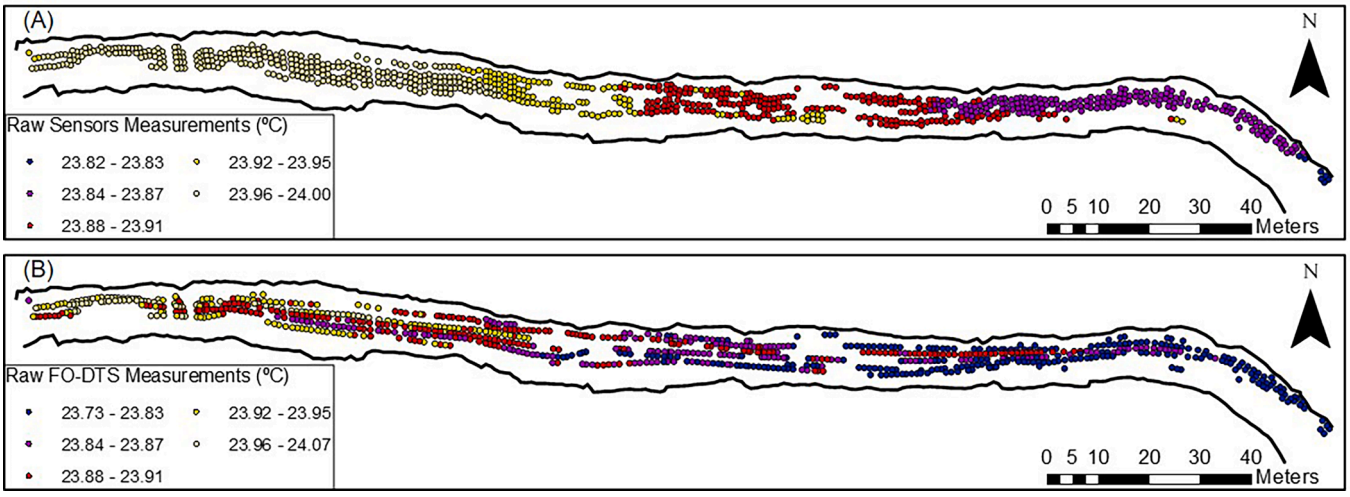

Fig. 5. Spatial distribution of the raw temperature sensor measurements (ºC) (A) and the spatial distribution of the FO-DTS measurements (ºC) at closely matching locations (B).

period. These two different measurement methods were able to map significant spatial variability in stream-water temperature, which was unexpected due to the relatively fast flowing stream water and turbulent mixing.

3.2.2. *Regression analysis*

The spatial threshold value of 0.5 m (noted above) was used to identify paired measurement locations for the two methods. The number of data points using the 0.5 m threshold was 818 compared to 1479 total data points. The temperature values measured with the two methods represented mainly the temperature of the stream-water column after removing the FO-DTS measurements from all locations that were buried in the streambed sediments and locations that were exposed to sun heating or were partly exposed to air temperature. Fig. 6 illustrates that the regression lines for all poles consistently fell below the 1:1 line indicating that FO-DTS observations were consistently lower than the corresponding temperature sensor measurements. This was attributed to a difference in the calibration between the two methods. The FO-DTS was calibrated to a slightly lower temperature standard relative to the individual temperature sensors. The regression between each pole and the paired FO-DTS measurements showed consistent and linear positive correlations (Fig. 6). The coefficient of determination (R^2) ranged between 0.71 and 0.83 and the slopes of the regressions ranged between 0.91 and 1.45. Each of these correlations were impacted by moderate

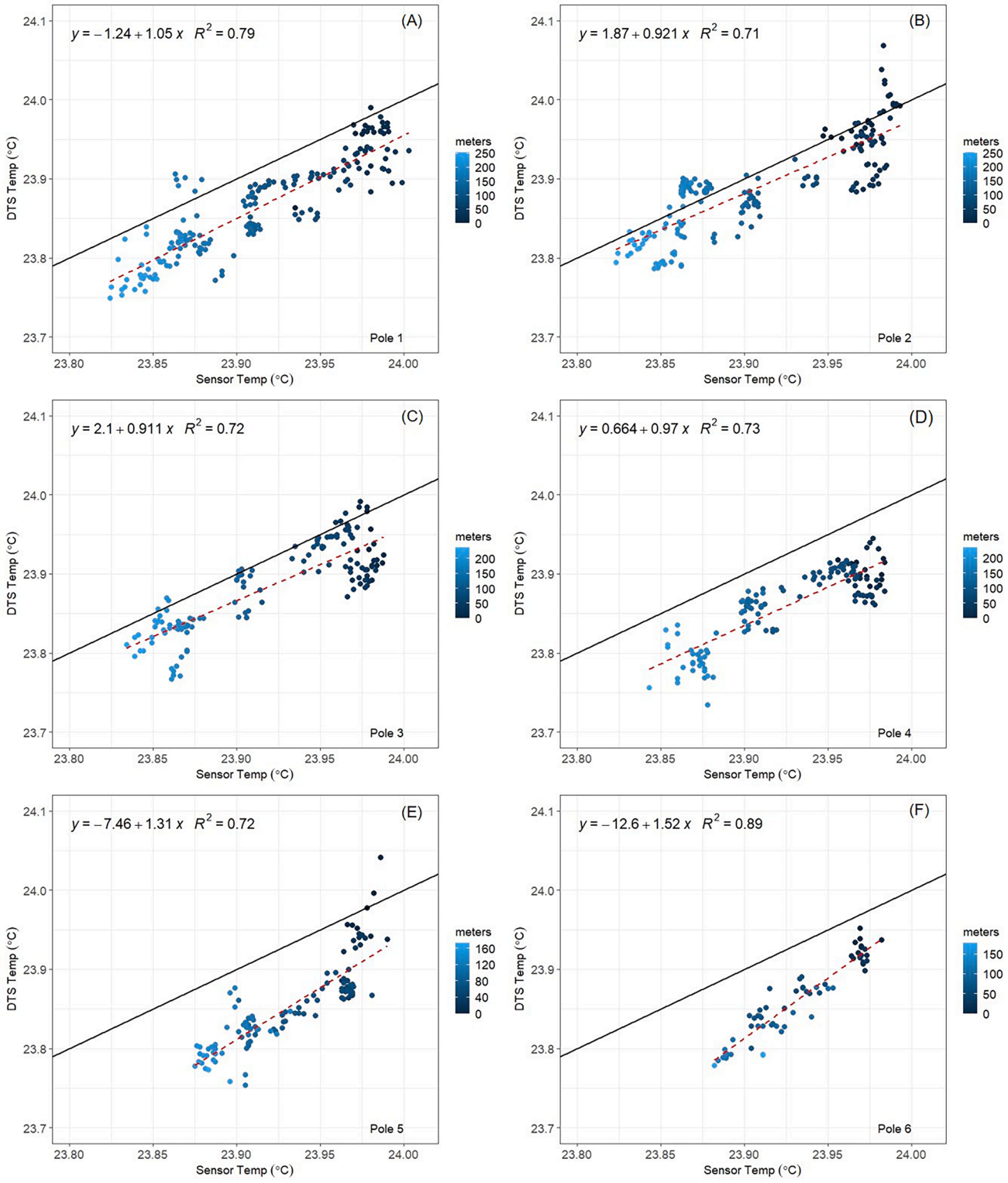

Fig. 6. Regression between the temperature sensor array measurements and the matching FO-DTS measurements for each of the individual sensor locations including (A) Pole-1, (B) Pole-2, (C) Pole-3, (D) Pole-4, (E) Pole-5, and (F) Pole-6. The dashed line in each plot is the best-fit regression model, while the solid line is the 1:1 line.

data scatter, and the amount of scatter and the R^2 values were similar for most of the poles except pole 6, which had the highest slope and intercept. Despite the scatter, the regressions were significant, and the measurements using these two methods were comparable. Spatial information was also represented in these method correlation plots using the color scale. The zero in the legend represents the location closest to the upstream boundary, and the color scale varies with increasing distance from upstream to the downstream boundary of the study reach (Fig. 6). The regression results show a consistent trend with cooler temperatures in the upstream and warmer temperature in the downstream, as observed in the raw dataset (Fig. 5).

The regression equation slopes were close to unity (3 to 9%

deviation) for poles 1 through 4 (Fig. 6). Pole 5 and 6 had larger deviations of the slope from unity. These two poles were closer to the south bank, which had the shallower water depth, some sediment bars, or islands, and some fallen trees. The north bank had a somewhat deeper water depth (relative to the south bank) suggesting that the thalweg runs near the north bank. The increases in regression equation slopes above unity for poles 5 and 6 were attributed to the difficulties in measurement of shallow water temperature near the south bank of the EFPC. Therefore, we posit that poles 5 and 6 had a larger measurement error compared to the other four poles due to the limited stream-water depth. Additionally, each of the RBR Solo temperature sensors had different accuracy and precision as the sensors were calibrated in different times. Another issue with direct comparison of the two methods was that each of the measurements for the two methods had slightly different spatial locations (horizontally and vertically), and the two spatial surveys had a different time resolution. Although the times and locations of measurements were coupled as closely as possible, the spatial and temporal variability in the measurements between these survey methods may have added to the uncertainty in the absolute temperature of the two methods.

Similar to the individual poles, the regression including all poles and all matching FO-DTS measurements showed a positive linear correlation (Fig. 7) indicating a strong correlation between the two datasets. However, the R^2 value of the regression including all poles and the all matching FO-DTS measurements was 0.62, which was less than those of the individual pole regression results. The increase in the data scatter for the regression including all poles, relative to the individual pole regression results, confirms that in-stream location measurement conditions impacted the correlation between these two measurement types. For example, the above noted proximity to the stream bank or stream-water depth limitations could have impacted these measurements. However, the relative amounts of data scatter were not variable with noticeable trends along the length of the stream reach (i.e., color scale for measurement location), and this relative consistency in amount of scatter along the stream channel direction seemed to be consistent between each of the individual pole data sets (Fig. 6) and the combined data set (Fig. 7).

3.2.3. Histogram of the differences

The average ± standard deviation of the temperature sensors survey was 23.91 ± 0.04 °C and of the FO-DTS survey was 23.87 ± 0.05 °C. The average ± standard deviation of the difference between the sensors and paired FO-DTS measurements was 0.05 °C ± 0.04 °C (Fig. 8). The minimum difference value was −0.09 °C, and the maximum difference value was 0.15 °C. The accuracy of the FO-DTS method was ± 0.05 °C − 0.10 °C, and therefore all difference values within this range or below ± 0.05 °C are considered biased and values greater than ± 0.10 °C are considered significant. The histogram shows that more than 95% of the

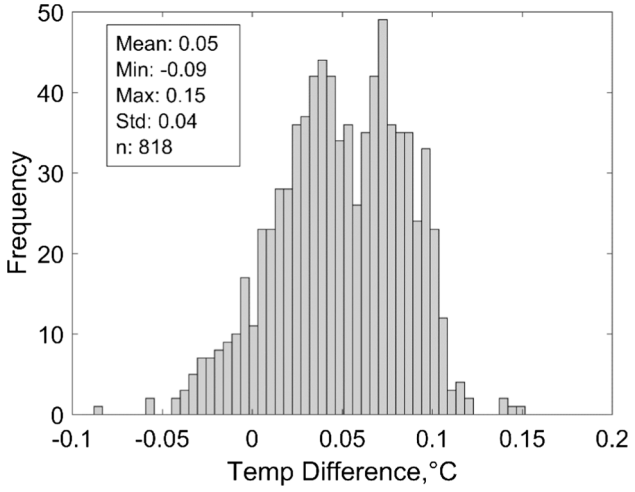

Fig. 8. Histogram of the difference between the temperature sensor array measurements and the matching FO-DTS measurements.

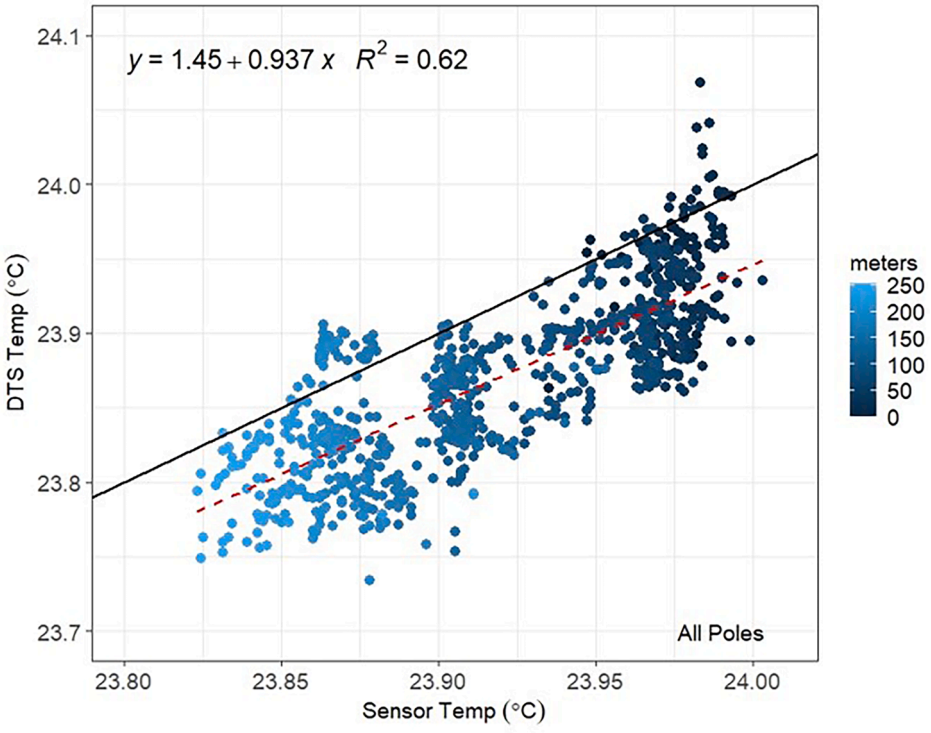

Fig. 7. Regression between the temperature sensor array measurements and the matching FO-DTS measurements for all data collection poles combined. The dashed line in each plot is the best-fit regression model, while the solid line is the 1:1 line.

differences were within the accuracy of the FO-DTS method, and only 5% were significant. The shape of the distribution of the differences between the two methods was consistent with a normally distributed variable, which determines that the distributions of the two datasets were close to normality. These results confirmed the null hypothesis that the two spatial stream-water temperature survey methods were similar, and this was also consistent with the above noted positive correlation results between the two methods.

3.2.4. Geostatistical analysis

Contour maps of the temperature sensor measurements and the paired FO-DTS measurements were created using Empirical Bayesian Kriging (Fig. 9). The trend of the spatial distribution followed closely the trend of the raw data for both measurement methods (Fig. 5), with higher temperatures mainly in the downstream and cooler temperatures in the upstream portions of the study reach. The mapped trends and variability was highly comparable between the two different measurement methods. Whereas, there does appear to be more variability in the temperature contour distributions for the map generated using the FO-DTS data.

Contour maps of the standard error of the kriging predictions generated using the temperature sensor measurements and the paired FO-DTS measurements are also presented (Fig. 10). The standard error of the prediction varied, and increased away from the measurement locations and close to the creek banks for both methods. The center of the channel generally had low error for both methods even though the low error along the center was not as consistently distributed for the FO-DTS method results. The standard error for the temperature sensor method was approximately an order of magnitude lower than that for the FO-DTS method, mainly because the measuring points for the temperature sensor method were evenly spaced and more data points were removed from the FO-DTS measurements. However, the standard error for both methods was low (ranging between 0.002 °C and 0.008 °C for the temperature sensor method and 0.03 °C and 0.039 °C for the FO-DTS method) compared to the accuracy of the two methods, suggesting that those errors were not significant.

Fig. 11 presents difference maps for examining the spatial distribution of the difference between the two temperature survey measurement approaches. Fig. 11a presents the map of differences between the Empirical Bayesian kriging maps shown in Fig. 9 (i.e., temperature sensor map minus FO-DTS map). The difference between the two spatial maps ranged between −0.08 °C and 0.15 °C. About 90.6% of the differences were less than 0.1 °C, and only 9.4% of the differences was greater than 0.1 °C, which therefore were considered significant and represented the measurable differences between the two methods. The locations of the larger temperature differences were mainly adjacent to the south bank in the upstream and between 0-m and 12.5-m in the downstream, where the stream water depth was shallower, and the measurement error of the temperature sensor was higher, as discussed above. Those locations with larger differences were consistent with the results presented in Fig. 11b, which is the difference map of the raw data that were shown in Fig. 5. The difference between the raw temperature sensor and FO-DTS measurements (Fig. 11b) showed spatially variable differences along the study reach with relatively higher differences (ranged between 0.12 °C and 0.16 °C) located along pole 6 close the south bank, and there were also a few locations of larger differences along pole 1 (i.e., close to the north bank) at meter 165 from the downstream boundary of the study reach. The increased measurement difference locations that were closer to the stream banks were also consistent with the increased regression slope deviations from unity for pole 5 and pole 6 (Fig. 6), and those locations were also consistent with the locations of the elevated standard error of the kriging prediction (Fig. 10). As discussed previously, the south bank had a shallower stream-water column, and therefore the temperature measured along pole 6 was likely affected by the warmer air temperatures. These results illustrate the potential limitations in the comparability of these two stream-water temperature survey methods, which includes locations near stream banks and where stream water depth is low. In fact, low flow or low water depth limitations or thresholds for the applicability of these methods might be considered, as well.

Fine spatial and temporal scales are often needed to monitor hyporheic zone interaction heterogeneity for applications such as quantifying solute transport, nutrient cycling, ecosystem assessment, and defining thermal refugia in streams and lakes. FO-DTS can provide a continuous measurement through a single fiber that are analogous to thousands of traditional temperature sensors with a fixed accuracy and precision along the cable. However, FO-DTS can be challenging to install in streams like EFPC where streambed bathymetry is variable due to the outcropping bedrock. FO-DTS is also relatively costly, data collection in remote areas is challenging due to continuous power source requirements, installation can be complex, the fiber is fragile and can be easily strained or broken, the calibration process can be extremely difficult, and the analysis can be complex and convoluted.

Some of the advantages of the temperature sensor array was its flexibility, low cost, ease of implementation, and ability to standardize the depth of measurement, which was not possible for the FO-DTS cable due to the variable stream bathymetry and exposed bedrock. The array structure also provided the flexibility to add more temperature sensors to achieve a finer resolution of the spatial coverage of temperature measurements. However, the method required more time to collect the

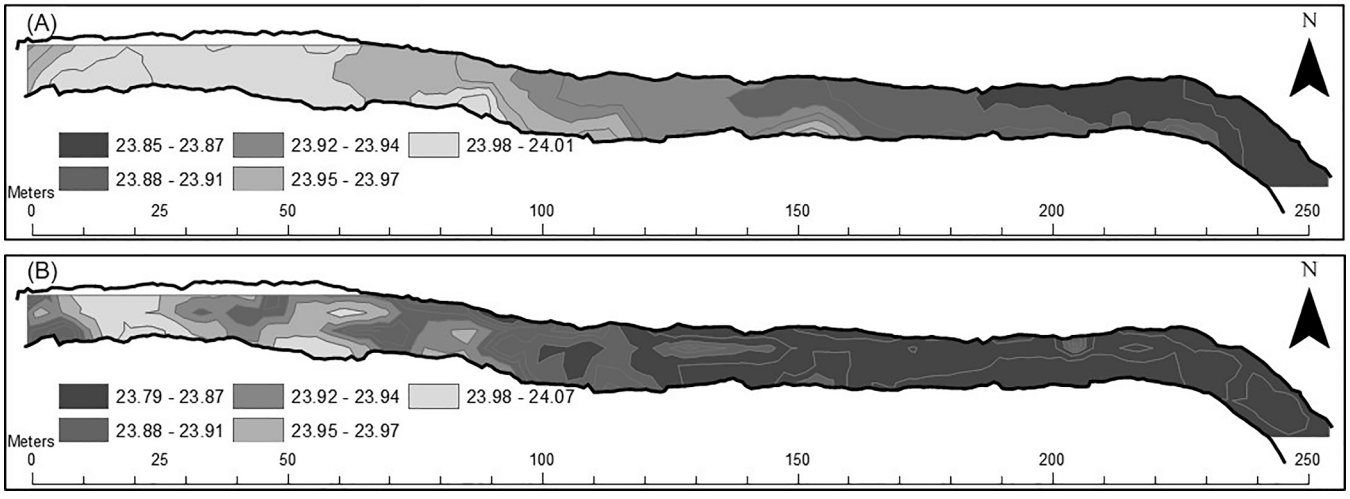

Fig. 9. Empirical Bayesian Kriging distribution of the temperature sensor array measurements (A) and FO-DTS measurements (B).

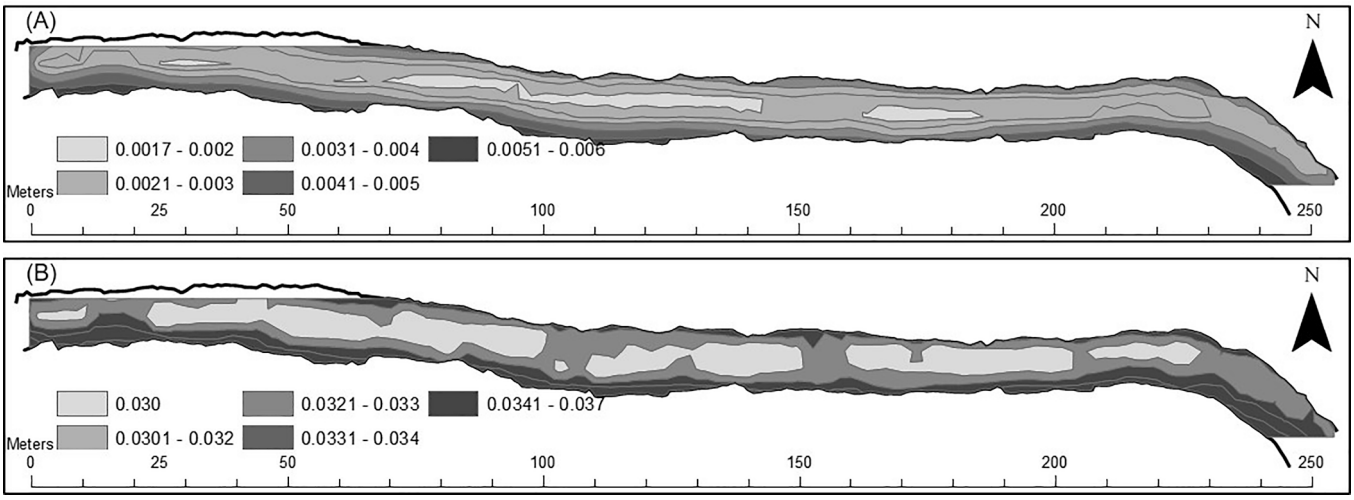

Fig. 10. Standard error of kriging prediction for the temperature sensor array measurements (A) and FO-DTS measurements (B).

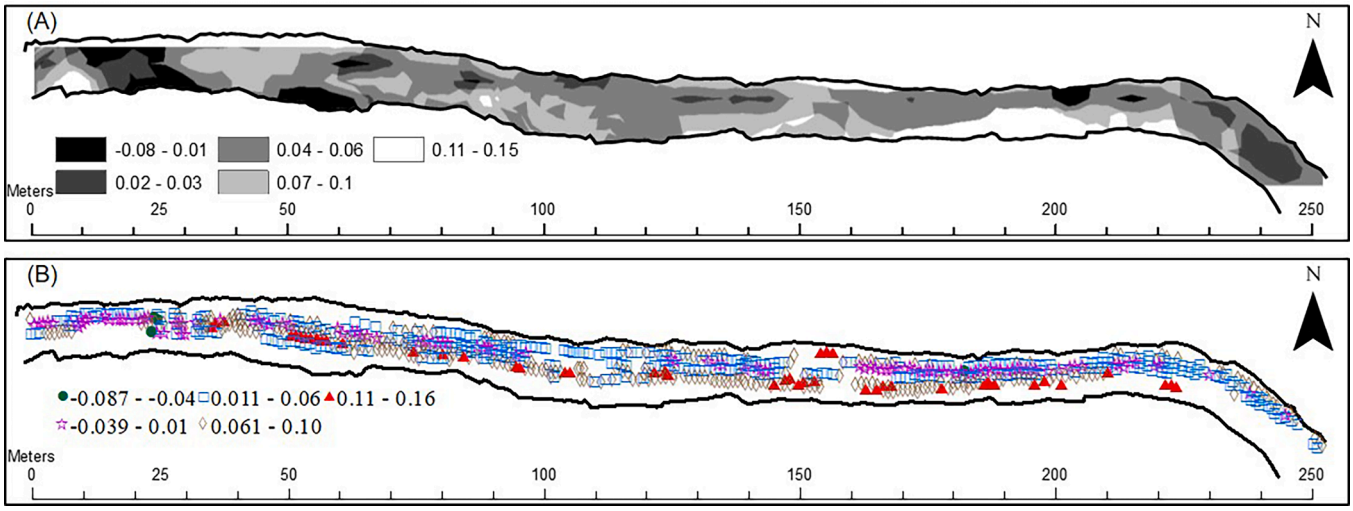

Fig. 11. Kriging map of the difference between the temperature sensor array kriging map and the FO-DTS kriging map (A), and map of the differences between the sensor array temperature and FO-DTS paired temperature measurement values (differences of the raw values) (B).

spatial distribution of data compared to the FO-DTS, and was not readily repeatable over time for monitoring, which is an advantage of the FO-DTS method if the installed cable distribution can be secured for some time. Data implementation and analysis was also less complex with the temperature sensors, though implementing the method required continuous labor throughout the temperature survey.

4. Summary and conclusions

In this study, we developed a simple array of highly-sensitive temperature sensors to measure the spatial temperature distribution within a stream reach, and the approach could be extended to measurement of streambed sediment temperatures by inserting the sensors into unconsolidated sediments at each measurement location. Moving a transect of highly-sensitive temperature sensors along the stream channel produced a 1 m by 1 m spatial survey of the stream water. The thermal sensors spatial survey was directly compared to a survey method using FO-DTS within the identical study reach area by identifying co-located measurement locations within the data sets of each method. The regression results between the FO-DTS measurements and the matching temperature sensor measurements showed correlations with R^2 values ranging between 0.71 and 0.83 for the individual temperature sensor poles and 0.62 for all poles combined. The regression equations were consistently positive with slopes close to 1, which confirmed the comparability and consistency of these two temperature surveying methods. Correlation differences from 1-to-1 were larger for measurements in shallower water near the south stream bank.

Comparison of these mapped spatial distributions showed similar trends between the two methods with warmer temperatures at the downstream and cooler temperatures at the upstream portions of the study reach. Geostatistical map prediction standard errors were generally low, but largest errors were along the edges of the stream banks where stream water was shallow and access limitations decreased data density. The differences between the methods were also mapped (temperature sensor measurements minus FO-DTS measurements), which showed that only 16% of the difference values exceeded the accuracy of the two methods. Further, the location of these significant differences were primarily along the south stream bank. These results all suggest that method comparability and measurement limitations likely occur in less accessible and shallower water depths along stream banks. Despite this limitation, the majority of the measurement locations were directly comparable, and both methods resulted in similar high-resolution spatial surveys of stream-water temperature despite the low amount of temperature differences.

These results generally support the practical utility of using the temperature sensor method as an alternative to the use of FO-DTS in streams where conditions are not amenable to application of the FO-DTS method. This study illustrated that using an array of several individual temperature sensors can provide a practical alternative to FO-DTS for spatial characterization of low order streams, providing slightly lower spatial and temporal resolution, but with higher accuracy of temperature measurement, with greater simplicity, and with a broader range of conditions where it may be applied. Although the two methods were fit to measure the water column temperature, limitations may exist to use the two methods to measure the distributed temperature of the sediment in similar streams with locations of bedrock outcrop along the streambed and little or no unconsolidated sediment lining the streambed. The mobile array of point temperature measurements developed herein can be used for surveying spatially distributed stream temperatures, which provides a comparable approach to the FO-DTS for characterization and monitoring along stream and river corridors.

Declaration of Competing Interest

The authors declare that they have no known competing financial interests or personal relationships that could have appeared to influence the work reported in this paper.

Acknowledgements

This work was supported by the Department of Energy (DOE) Minority Serving Institution Partnership Program (MSIPP) managed by the Savannah River National Laboratory. Additional support was provided by the USDA National Institute of Food and Agriculture (Hatch project 1023257). A portion of this research was sponsored by the Office of Biological and Environmental Research within the Office of Science of the U.S. DOE, as part of the Critical Interfaces Science Focus Area project at the Oak Ridge National Laboratory (ORNL). We thank CTEMPs, funded by the National Science Foundation (EAR awards 1832109 and 1832170), for timely and effective provision of experimental design support, logistical support and equipment for the project. Access to the temperature data are provided at CTEMPS.org, and DOE will provide public access to the EFPC data collected for federally sponsored research in accordance with the DOE Public Access Plan (http://energy.gov/downloads/doe-public-access-plan). ORNL is managed by UT-Battelle, LLC under Contract No. DE-AC05-00OR22725 with DOE. We appreciate the assistance of Cara Walter, Julie Huff, Ahmed Elaksher, Kenneth Lowe, Chris Kubicki, and Autumn Pearson.

References

Assendelft, R.S., van Meerveld, H.J., 2019. A low-cost, multi-sensor system to monitor temporary stream dynamics in mountainous headwater catchments. Sensors 19 (21), 4645.

Bertrand, G., Siergieiev, D., Ala-Aho, P., Rossi, P.M., 2014. Environmental tracers and indicators bringing together groundwater, surface water and groundwater-dependent ecosystems: importance of scale in choosing relevant tools. Environ. Earth Sci. 72 (3), 813–827.

Bond, R.M., Stubblefield, A.P., Van Kirk, R.W., 2015. Sensitivity of summer stream temperatures to climate variability and riparian reforestation strategies. J. Hydrol.: Reg. Stud. 4, 267–279.

Briggs, M.A., Buckley, S.F., Bagtzoglou, A.C., Werkema, D.D., Lane, J.W., 2016. Actively heated high-resolution fiber-optic-distributed temperature sensing to quantify streambed flow dynamics in zones of strong groundwater upwelling. Water Resour. Res. 52 (7), 5179–5194.

Brooks, S., Lowe, K., 2019. [Data Set] East Fork Poplar Creek Discharge at Kilometer 5.4 Water Year 2019.

Brooks, S.C., Southworth, G.R., 2011. History of mercury use and environmental contamination at the Oak Ridge Y-12 Plant. Environ. Pollut. 159 (1), 219–228. https://doi.org/10.1016/j.envpol.2010.09.009.

Brooks, S.C. et al., 2018. Intraday water quality patterns in East Fork Poplar Creek with an emphasis on mercury and monomethylmercury. Oak Ridge National Lab.(ORNL), Oak Ridge, TN (United States).

Caldwell, T.G., Wolaver, B.D., Bongiovanni, T., Pierre, J.P., Robertson, S., Abolt, C., Scanlon, B.R., 2020. Spring discharge and thermal regime of a groundwater dependent ecosystem in an arid karst environment. J. Hydrol. 587, 124947. https://doi.org/10.1016/j.jhydrol.2020.124947.

Collier, M.W., 2008. Demonstration of fiber optic distributed temperature sensing to differentiate cold water refuge between ground water inflows and hyporheic exchange.

Coluccio, K., Morgan, L.K., 2019. A review of methods for measuring groundwater–surface water exchange in braided rivers. Hydrol. Earth Syst. Sci. 23 (10), 4397–4417.

Conant, B., 2004. Delineating and quantifying ground water discharge zones using streambed temperatures. Groundwater 42 (2), 243–257.

Conant, B., Robinson, C.E., Hinton, M.J., Russell, H.A.J., 2019. A framework for conceptualizing groundwater-surface water interactions and identifying potential impacts on water quality, water quantity, and ecosystems. J. Hydrol. 574, 609–627.

Constantz, J., 2008. Heat as a tracer to determine streambed water exchanges. Water Resour. Res. 44, W00D10. https://doi.org/10.1029/2008WR006996.

Constantz, J., Stonestrom, D.A., Stewart, A.E., Niswonger, R.G., Smith, T.R., 2001. Evaluating streamflow patterns along seasonal and ephemeral channels by monitoring diurnal variations in streambed temperature. Water Resour. Res. 37 (2), 317–328.

Culbertson, C.W., Huntington, T.G., Caldwell, J.M., O'Donnell, C., 2013. Evaluation of aerial thermal infrared remote sensing to identify groundwater-discharge zones in the Meduxnekeag River, Houlton, Maine. US Department of the Interior, US Geological Survey.

Cunningham, M., Pounds, L., 1991. Resource Management plan for the Oak Ridge Reservation. Volume 28, Wetlands on the Oak Ridge Reservation. Oak Ridge National Lab.(ORNL), Oak Ridge, TN (United States).

Demers, J.D., Blum, J.D., Brooks, S.C., Donovan, P., Riscassi, A.L., Miller, C.L., Zheng, W., Gu, B., 2018. Hg isotopes reveal in-stream processing and legacy inputs in East Fork Poplar Creek, Oak Ridge, Tennessee, USA. Environ. Sci. Processes Impacts 20 (4), 686–707.

Dole-Olivier, M.-J., Wawzyniak, V., Des Chatelliers, M.C., Marmonier, P., 2019. Do thermal infrared (TIR) remote sensing and direct hyporheic measurements (DHM) similarly detect river-groundwater exchanges? Study along a 40 km-section of the Ain River (France). Sci. Total Environ. 646, 1097–1110.

Dugdale, S.J., 2016. A practitioner's guide to thermal infrared remote sensing of rivers and streams: recent advances, precautions and considerations. Wiley Interdisciplinary Reviews: Water 3 (2), 251–268.

Dugdale, S.J., Kelleher, C.A., Malcolm, I.A., Caldwell, S., Hannah, D.M., 2019. Assessing the potential of drone-based thermal infrared imagery for quantifying river temperature heterogeneity. Hydrol. Process. 33 (7), 1152–1163.

Dzara, J.R., Neilson, B.T., Null, S.E., 2019. Quantifying thermal refugia connectivity by combining temperature modeling, distributed temperature sensing, and thermal infrared imaging. Hydrol. Earth Syst. Sci. 23 (7), 2965–2982.

Folegot, S., 2018. A Risk Assessment Framework for Quantifying Drought Impacts on Thermal and Water Extremes. University of Birmingham.

Fullerton, A.H., Torgersen, C.E., Lawler, J.J., Steel, E.A., Ebersole, J.L., Lee, S.Y., 2018. Longitudinal thermal heterogeneity in rivers and refugia for coldwater species: effects of scale and climate change. Aquat. Sci. 80 (1) https://doi.org/10.1007/s00027-017-0557-9.

Gendaszek, A., 2011. Thermal profiles for selected river reaches in the Stillaguamish River Basin, Washington, August 2011. USGS Data Ser, 654.

Hall, A., Chiu, Y.C., Selker, J.S., 2020. Coupling high-resolution monitoring and modelling to verify restoration-based temperature improvements. River Res. Appl. 36 (8), 1430–1441.

Hare, D.K., Briggs, M.A., Rosenberry, D.O., Boutt, D.F., Lane, J.W., 2015. A comparison of thermal infrared to fiber-optic distributed temperature sensing for evaluation of groundwater discharge to surface water. J. Hydrol. 530, 153–166.

Hausner, M.B., Suárez, F., Glander, K.E., Giesen, N.V.d., Selker, J.S., Tyler, S.W., 2011. Calibrating single-ended fiber-optic Raman spectra distributed temperature sensing data. Sensors 11 (11), 10859–10879.

Huff, J.A., 2009. Monitoring river restoration using fiber optic temperature measurements in a modeling framework.

Keery, J., Binley, A., Crook, N., Smith, J.W.N., 2007. Temporal and spatial variability of groundwater–surface water fluxes: development and application of an analytical method using temperature time series. J. Hydrol. 336 (1-2), 1–16.

Kurth, A.M., Dawes, N., Selker, J., Schirmer, M., 2013. Autonomous distributed temperature sensing for long-term heated applications in remote areas. Geosci. Instrum. Methods Data Syst. 2 (1), 71–77.

Kurylyk, B.L., Irvine, D.J., Bense, V.F., 2019. Theory, tools, and multidisciplinary applications for tracing groundwater fluxes from temperature profiles. Wiley Interdisciplinary Reviews: Water 6 (1) e1329.

Lautz, L.K., Kranes, N.T., Siegel, D.I., 2010. Heat tracing of heterogeneous hyporheic exchange adjacent to in-stream geomorphic features. Hydrol. Process. 24 (21), 3074–3086.

Lee, D.R., 1985. Method for locating sediment anomalies in lakebeds that can be caused by groundwater flow. J. Hydrol. 79 (1-2), 187–193.

Liu, C., Liu, J., Hu, Y., Wang, H., Zheng, C., 2016. Airborne thermal remote sensing for estimation of groundwater discharge to a river. Groundwater 54 (3), 363–373.

Lowry, C.S., Walker, J.F., Hunt, R.J., Anderson, M.P., 2007. Identifying spatial variability of groundwater discharge in a wetland stream using a distributed temperature sensor. Water Resour. Res. 43 (10).

Mamer, E.A., Lowry, C.S., 2013. Locating and quantifying spatially distributed groundwater/surface water interactions using temperature signals with paired fiber-optic cables. Water Resour. Res. 49 (11), 7670–7680.

Marcus, W.A., 2012. Remote sensing of the hydraulic environment in gravel-bed rivers. Gravel-bed rivers: Processes, tools, environments: 259-285.

Markus, N., Helena, M., 2002. Open Source GIS: A Grass GIS Approach. Kluwer Academic Publication, Boston.
Marruedo Arricibita, A.I., 2018. Upscaling of Lacustrine Groundwater Discharge by Fiber Optic Distributed Temperature Sensing and Thermal Infrared imaging.
Mohamed, R.A.M., S.C. Brooks, C.-H. Tsai, T. Ahmed, D.F. Rucker, A.L. Ulery, E.M. Pierce, and K.C. Carroll, 2021. Geostatistical Interpolation of Streambed Hydrologic Attributes with Addition of Left Censored Data and Anisotropy. Journal of Hydrology, Volume 599, 126474, ISSN 0022-1694, https://doi.org/10.1016/j.jhydrol.2021.126474.
Neilson, Bethany, Hatch, Christine, Ban, Heng, Tyler, Scott, 2010. Solar radiative heating of fiber-optic cables used to monitor temperatures in water. Water Resour. Res. 46, W08540 https://doi.org/10.1029/2009WR008354.
Pai, H., Malenda, H.F., Briggs, M.A., Singha, K., González-Pinzón, R., Gooseff, M.N., Tyler, S.W., 2017. Potential for small unmanned aircraft systems applications for identifying groundwater-surface water exchange in a meandering river reach. Geophys. Res. Lett. 44 (23) https://doi.org/10.1002/grl.v44.2310.1002/2017GL075836.
Read, T., Bour, O., Selker, J.S., Bense, V.F., Borgne, T.L., Hochreutener, R., Lavenant, N., 2014. Active-distributed temperature sensing to continuously quantify vertical flow in boreholes. Water Resour. Res. 50 (5), 3706–3713.
Roshan, H., Young, M., Andersen, M.S., Acworth, R.I., 2014. Limitations of fibre optic distributed temperature sensing for quantifying surface water groundwater interactions. Hydrol. Earth Syst. Sci. Discuss. 11 (7), 8167–8190.
Rucker, D., C.-H. Tsai, K.C. Carroll, S.C. Brooks, E. Pierce, A. Ulery, and C. DeRolph, 2021. Bedrock Architecture, Soil Structure, and Hyporheic Zone Characterization Combining Electrical Resistivity and Induced Polarization Imaging. Applied Geophysics, Volume 188, 104306, ISSN 0926-9851, doi:10.1016/j.jappgeo.2021.104306.
Schornberg, C., Schmidt, C., Kalbus, E., Fleckenstein, J.H., 2010. Simulating the effects of geologic heterogeneity and transient boundary conditions on streambed temperatures—Implications for temperature-based water flux calculations. Adv. Water Resour. 33 (11), 1309–1319.
Scotch, C.G., Murgulet, D., Constantz, J., 2021. Time-series temperature analyses indicate conduction and diffusion are dominant heat-transfer processes in fine sediment, low-flow streams. Sci. Total Environ. 768, 144367.
Selker, J.S., Thévenaz, L., Huwald, H., Mallet, A., Luxemburg, W., van de Giesen, N., Stejskal, M., Zeman, J., Westhoff, M., Parlange, M.B., 2006c. Distributed fiber-optic temperature sensing for hydrologic systems. Water Resour. Res. 42 (12).
Selker, J., van de Giesen, N., Westhoff, M., Luxemburg, W., Parlange, M.B., 2006a. Fiber optics opens window on stream dynamics. Geophys. Res. Lett. 33 (24).
Selker, J., van de Giesen, N., Westhoff, M., Luxemburg, W., Parlange, M.B., 2006b. Fiber optics opens window on stream dynamics. Geophys Res Lett 33 (24), L24401.
Sebok, Eva, Duque, Carlos, Engesgaard, Peter, Boegh, Eva, 2015. Application of Distributed Temperature Sensing for coupled mapping of sedimentation processes and spatio-temporal variability of groundwater discharge in soft-bedded streams. Hydrol. Process. 29, 3408–3422. https://doi.org/10.1002/hyp.10455.
Selker, J., Selker, F., Huff, J., Short, R., Edwards, D., Nicholson, P., Chin, A., 2014. Practical strategies for identifying groundwater discharges into sediment and surface water with fiber optic temperature measurement. Environ. Sci. Processes Impacts 16 (7), 1772–1778.
Shanafield, M., Bourke, S.A., Zimmer, M.A., Costigan, K.H., 2021. An overview of the hydrology of non-perennial rivers and streams. Wiley Interdisciplinary Rev.: Water 8 (2) e1504.
Sorey, M.L., 1971. Measurement of vertical groundwater velocity from temperature profiles in wells. Water Resour. Res. 7 (4), 963–970.
Stallman, R.W., 1965. Steady one-dimensional fluid flow in a semi-infinite porous medium with sinusoidal surface temperature. J. Geophys. Res. 70 (12), 2821–2827.
Stoneman, D.A., Constantz, J., 2003. Heat as a tool for studying the movement of ground water near streams, 1260. US Department of the Interior, US Geological Survey.
Suárez, F., Dozier, J., Selker, J.S., Hausner, M.B., Tyler, S.W., 2011. Heat transfer in the environment: development and use of fiber-optic distributed temperature sensing. INTECH Open Access Publisher Rijeka.
Torgersen, C.E., Faux, R.N., McIntosh, B.A., Poage, N.J., Norton, D.J., 2001. Airborne thermal remote sensing for water temperature assessment in rivers and streams. Remote Sens. Environ. 76 (3), 386–398.
Tyler, S.W., Selker, J.S., Hausner, M.B., Hatch, C.E., Torgersen, T., Thodal, C.E., Schladow, S.G., 2009. Environmental temperature sensing using Raman spectra DTS fiber-optic methods. Water Resour. Res. 45 (4).
Tyler, S.W., Holland, D.M., Zagorodnov, V., Stern, A.A., Sladek, C., Kobs, S., White, S., Suárez, F., Bryenton, J., 2013. Using distributed temperature sensors to monitor an Antarctic ice shelf and sub-ice-shelf cavity. J. Glaciol. 59 (215), 583–591.
Vaccaro, J.J., Maloy, K.J., 2006. A thermal profile method to identify potential groundwater discharge areas and preferred salmonid habitats for long river reaches.
White, D.S., Elzinga, C.H., Hendricks, S.P., 1987. Temperature patterns within the hyporheic zone of a northern Michigan river. J. North American Benthol. Society 6 (2), 85–91.
Winter, T.C., LaBaugh, J.W., Rosenberry, D.O., 1988. The design and use of a hydraulic potentiomanometer for direct measurement of differences in hydraulic head between groundwater and surface water. Limnol. Oceanogr. 33 (5), 1209–1214.